Are seismic waves robust enough to detect the presence of water in the lower part of the mantle transition zone?

Rabindranath Mondal[1,*], Gaurav Shukla[1], Swastika Chatterjee[1]

[1]National Centre for High-Pressure Studies and Department of Earth Sciences, Indian Institute of Science Education and Research Kolkata, Nadia 741246, West Bengal, India

Email: rm19rs089@iiserkol.ac.in

Abstract

The mantle transition zone (MTZ) is known to be potentially hydrated as laboratory experiments have shown that the two major mineral phases namely wadsleyite (β-M_2SiO_4; M: Mg, Fe) and ringwoodite (γ-M_2SiO_4; M: Mg, Fe) can accommodate significant amounts of water in the form of hydroxyl ions in their crystal structure. Direct in-situ evidence of the MTZ being (at least locally) hydrated has been derived from natural diamonds containing hydrous ringwoodite inclusions (Pearson 2014, Nature). Hence, in this study, we have investigated the crystal structure and the thermoelastic properties of Fe-bearing ringwoodite as a function of temperature, pressure, and water content (0 wt%, 1.56 wt%, 3.3 wt%) using a combination of first-principles density functional theory (DFT) and quasi-harmonic approximation (QHA). Our calculation reveals that hydration in general causes a reduction in the sound wave velocity of ringwoodite. However, the 'reduction' brought in by hydration is significantly suppressed at pressures corresponding to the lower part of the MTZ. Consequently, the sound wave velocities for the 1.56 wt% water-containing ringwoodite model is found to become very similar to the sound wave velocities of the anhydrous ringwoodite. However, when the water concentration is increased further to ~3.3 wt%, the pressure-induced suppression at lower MTZ pressures though present is not significant. These findings indicate that though seismic waves may not be able to precisely decipher the state of hydration of the lower part of MTZ when the water concentration is less than 1.56 wt%, it is still robust enough to locate regions of very high-water concentration ~ 3.3 wt%.

1. Introduction & Motivation:

- The Earth's mantle transition zone (MTZ) (at the depths of 410-660 km) is considered to serve as a water reservoir, primarily due to the ability of its main constituents, wadsleyite (β-$(Fe, Mg)_2SiO_4$), and ringwoodite (γ-$(Fe, Mg)_2SiO_4$) (refer to Figure 1), to store a significant amount of water within their crystal structure in the form of hydroxyl ions (-OH). It is estimated that wadsleyite can incorporate up to 3.3 wt.% H_2O, while ringwoodite can accommodate up to 2.2 wt.% H_2O (Kudoh et al., 2000; Frost, 2008). Water is known to enter into the Earth's interior via subduction and is released through volcanoes.

- Pearson et al. (2014) discovered ringwoodite inclusion with ~1.5 wt.% H_2O in an ultra-deep diamond, which demonstrates that the mantle transition zone is at least locally hydrated (refer to Figure 1(a)).

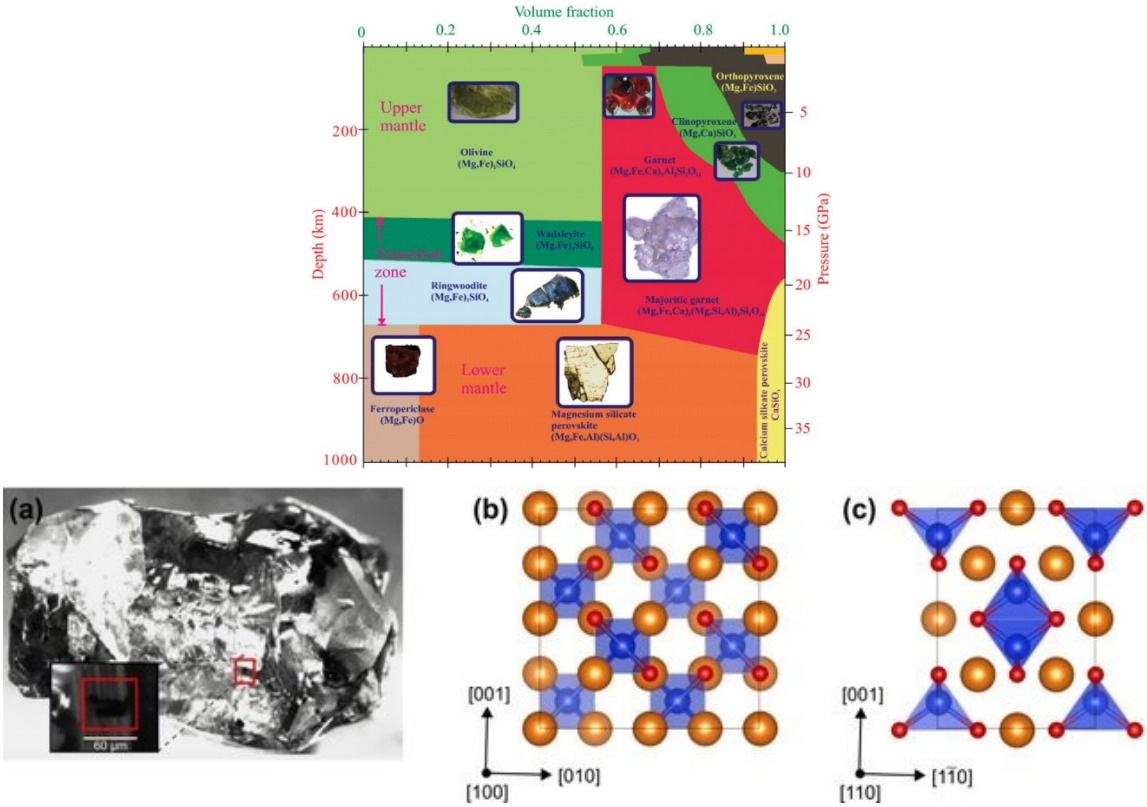

Figure 1: Upper panel: Mineral volume fractions of a pyrolite mantle (Frost, 2008); Lower panel: (a) Hydrous ringwoodite inclusions in natural diamond (Pearson et al., 2014). (b) & (c) ringwoodite crystal structure in different angles.

- The water content of the MTZ and its spatial distribution inside the Earth are essential because apart from giving us information about the structure and chemical composition of the mantle, it may hold vital clues regarding the geochemical recycling and the pattern of convection taking place in the mantle.
- In the case of ringwoodite, various experimental techniques, namely X-ray diffraction Brillion spectroscopy ultrasonic measurements, electrical conductivity measurements, mineral viscosity data, as well as theoretical first-principles have been employed to unravel the mechanism of water incorporation and estimate the amount of water potentially present in ringwoodite under MTZ conditions. However, the results are largely inconclusive, with a huge variation in the reported water content (~0.1 to 2.0 wt.%).
- One of the most powerful tools that gives us information about the state of hydration of the Earth's interior is seismology. Seismology exploits the fact that water incorporation affects the seismic wave velocities (Inoue et al., 1998; Jacobsen et al., 2004), which in turn may be used to decipher the water content of the mantle. However, apart from water, variations in temperature and Fe content may also influence the wave velocity at a given pressure.

- Therefore, we have investigated the cumulative effect of Fe and varying quantities of water on the elastic properties of ringwoodite under MTZ pressure and temperature conditions. Our aim was to probe the efficacy of seismic waves at detecting the state of hydration of the MTZ.

2. Computational Methodology:

- All calculations have been performed using first-principles density functional theory (DFT) (Hohenberg and Khon, 1964; Kohn and Sham, 1965) as implemented in the Vienna ab-initio simulation package (VASP) (Kresse and Hafner, 1993; Kresse and Furthmüller, 1996). We have used the projector-augmented-wave (PAW) (Blöchl,1994; Kresse and Joubert, 1999) implementation of DFT. Generalized gradient approximation (GGA) with Perdew–Burke–Ernzerhof (PBE) (Perdew et al., 1996) parametrization was chosen for determining the equilibrium crystal structure of anhydrous/hydrous Fe-containing ringwoodite. Additionally, the local density approximation (LDA) was employed for the pressure-volume equation of state calculations (Yu et al., 2008; Li et al., 2009; Panero, 2010; Núñez-Valdez et al., 2012), as it yields more accurate structural properties compared to GGA. The missing correlation effect at the Fe sites has been incorporated via LDA/GGA + U calculations, where U is the onsite coulomb repulsion (Hubbard, 1963).
- Thermodynamic properties have been estimated within quasiharmonic approximation (QHA) (Wallace, 1972) as implemented in qha python package (Qin et al., 2019). Force constant matrices were computed using density functional perturbation theory (DFPT) (Baroni et al., 2001) as implemented in VASP. These force constants were used to estimate the vibrational density of states (VDoS) for QHA implementation using PHONOPY code (Togo and Tanaka, 2015). Thermal bulk and shear moduli have been estimated using a semi-analytical method based on quasi-harmonic approximation (Wu and Wentzcovitch, 2011) as implemented in Cij python package (Luo et al., 2021).
- The free energy within QHA:

$$F(V,T) = U(V) + \sum_{qj} \frac{\hbar\omega_{qj}(V)}{2} + k_B T \sum_{qj} \ln\left(1 - \exp\left[-\frac{\hbar\omega_{qj}(V)}{k_B T}\right]\right)$$

  Where ω(V) is the phonon spectrum at volume V and U(V) is the static internal energy of the system. The second term is the zero-point energy and the last term is the thermal excitation energy.

3. Crystal Structure of Hydrous Ringwoodite:

Water incorporation in ringwoodite has been proposed to happen in three different ways, namely (i) Octahedral site vacancy charge compensated by two hydrogen ions (V_{Mg}" + 2H**), (ii) Mg atom substituted for Si in the tetrahedral site charge compensated by two hydrogen atoms (Mg_{Si}" + 2H**) and (iii) Vacancy at Si site charge compensated by four

protons (V_{Si}'''' + 4H****) (Verma and Karki, 2009). Relative energetics indicate that the ratio in which these defects may appear in a ringwoodite crystal is 64:10:25 (Panero, 2010).

Therefore, the defect structure with vacancy at a Mg site, charge compensated by two protons would be the most dominant mechanism by which water will be incorporated in the ringwoodite crystal structure. Si forms very strong covalent bonds with oxygen atoms, the creation of Si vacancies requires a significantly large amount of energy as compared to the creation of Mg vacancies (Chatterjee et al., 2012), and hence defect models involving vacancies at Si sites are less probable.

Water incorporation in 12.5% Fe-containing γ-Mg_2SiO_4.

We have investigated water incorporation in 12.5% Fe-containing ringwoodite, with special emphasis on the most dominant defect configuration involving one Mg site vacancy (1.56 wt.% H_2O), charge-balanced by two protons. Here each unit cell of ringwoodite contains two Fe atoms. It is to be noted that the moment we introduce two Fe ions, the equivalence of the M sites is lifted. The two Fe atoms can be distributed among the 16 M-octahedral sites (per unit cell) in several ways. For each of those configurations, one can create, the vacancy is any of the 14 remaining sites. Further complexity is brought in by the different ways in which one can place the two oxygen atoms around the vacant octahedral site. The lowest energy configuration of Fe-bearing hydrous ringwoodite is when the two iron atoms are close together with a distance of 2.417 Å. Both these Fe ions share edges with the vacant octahedra as can be seen in Figure 2(a).
The incorporation of 1 M-site vacancy per unit cell charge balanced by two protons culminates into a water concentration of 1.56 wt.%. Experimentally it has been suggested that the ringwoodite crystal structure can incorporate a much greater amount of water. This indicates that the vacancy concentration must be greater than one per unit cell. To accommodate a greater amount of water in our theoretical ringwoodite model, we have simulated a ringwoodite structure with two M-site vacancies per unit cell (3.3 wt.% H_2O). It has been seen that although the incorporation of 2 protons for each M-site vacancy takes care of the global charge neutrality, at the microscopic level, the vacant site is still charged (Das et al., 2022). As a result, it is expected that they would prefer to stay farther apart to reduce electrostatic repulsion. We have therefore placed the two vacancies per unit cell at the largest possible distance and varied the arrangement of the two Fe atoms per unit cell. Our total energy calculations find that each vacant octahedra finds one Fe atom as its neighbor as elucidated in Figure 2(b).

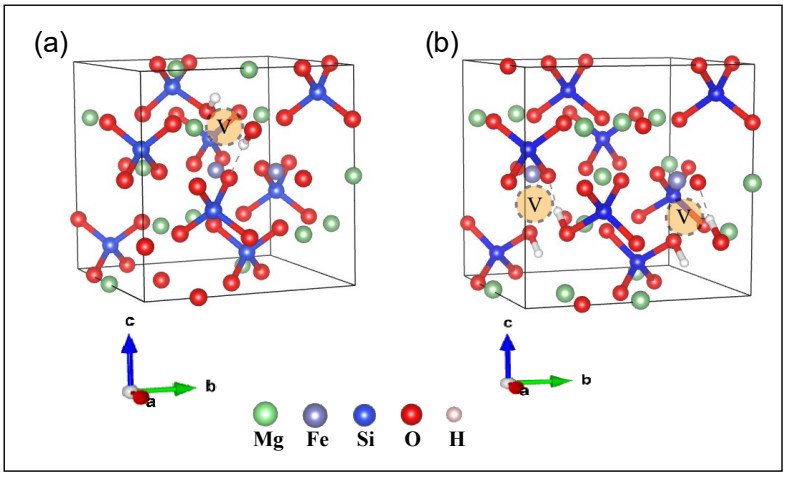

Figure 2: Crystal structure of 12.5% Fe containing hydrous ringwoodite. (a) Water content: 1.56 wt.% (b) water content: 3.3 wt.%.

4. Results:

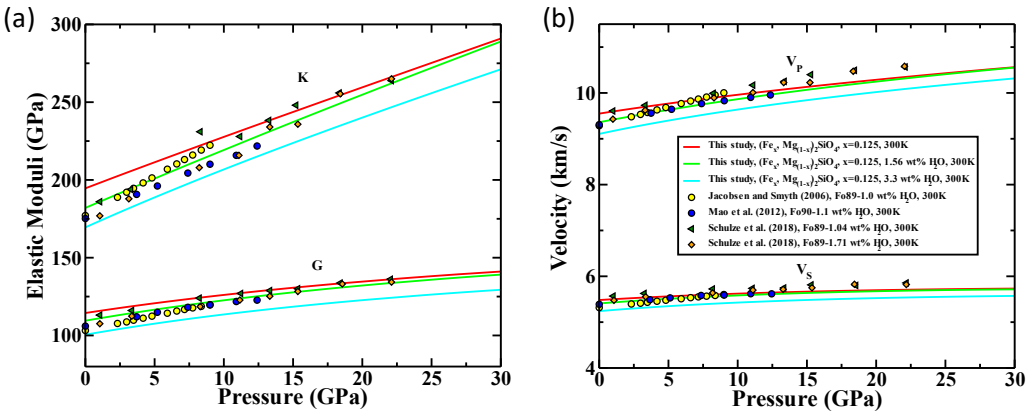

Figure 3: Elasticity of hydrous 12.5% Fe containing ringwoodite at 300 K as a function of pressure compared with previous experimental studies. (a) Bulk (K) and shear (G) moduli, (b) Compressional (V_P) and shear (V_S) wave velocities.

Since mantle minerals contain about 10% Fe (Fe/ (Fe + Mg)), it is important to look at the effect of both Fe and water on the elastic properties of ringwoodite. Also, it is to be noted that the MTZ is a region of high temperature and hence it is important to include the effect of temperature in the calculated elasticity. It is approximated that the temperature in the MTZ ranges between 1700 K and 2000 K (Ito and Katsura, 1989; Katsura et al., 2010). Therefore, we have determined the elastic properties of anhydrous and hydrous 12.5% Fe-containing ringwoodite at three different temperatures, namely 300 K (i.e., room temperature), 1700 K, and 2000 K. K, G, V_P, and V_S calculated at 300 K with previously published experimental data is presented in Figure 3. It is found that with the introduction of 1.56 wt.% water, there is in general a reduction in K and G. This reduction is highly pronounced at low pressure. However, with an increase in pressure, the difference (in K and G) between anhydrous ringwoodite and 1.56 wt.% water containing ringwoodite significantly decreases such that at pressures corresponding to the lower part of the MTZ

the two curves become almost indistinguishable. Our calculations find that at lower temperatures, namely 300 K, the bulk modulus of anhydrous ringwoodite is greater than the 1.56 wt.% water-containing ringwoodite by 6.5% at 0 GPa. Whereas at 30 GPa the same is 0.7%. Similarly, the shear modulus of the anhydrous phase is larger than the hydrous (1.56 wt.% H_2O) phase by 4.3% at 0 GPa and by 1.4% at 30 GPa. As temperature increases, this suppression is found to get arrested to a certain extent in the case of the bulk modulus, whereas it is found to get enhanced in the case of the shear modulus. Our calculations indicate that at 30 GPa, the bulk modulus of the anhydrous phase is larger than the hydrous (1.56 wt.% H_2O) phase by 0.9% at 1700 K and by 1.2% at 2000 K (shown in Figure 4). Whereas, at the same pressure, the shear modulus of the anhydrous phase is larger than that of the hydrous (1.56 wt.% H_2O) phase by 1.0% at 1700 K and by 0.8% at 2000 K. It is evident that the compressional (V_P) and shear (V_S) wave velocities, which are related to the K and G would also show similar trends.

To study the effect of larger water concentration on the elastic properties of ringwoodite, we considered a ringwoodite defect structure containing 2 vacancies and 4 protons per unit cell, which results in a water concentration of 3.3 wt.%. The values of K, G, V_P, and V_S as a function of pressure at 300 K are shown in Figure 3. Comparison with anhydrous ringwoodite shows that the reduction due to 3.3 wt.% H_2O incorporation in K, G, V_P, and V_S at 0 GPa is 12.90%, 12.17%, 4.64%, and 4.41% respectively. The same values at 30 GPa are 6.81%, 8.30%, 2.31% and 2.80% respectively.

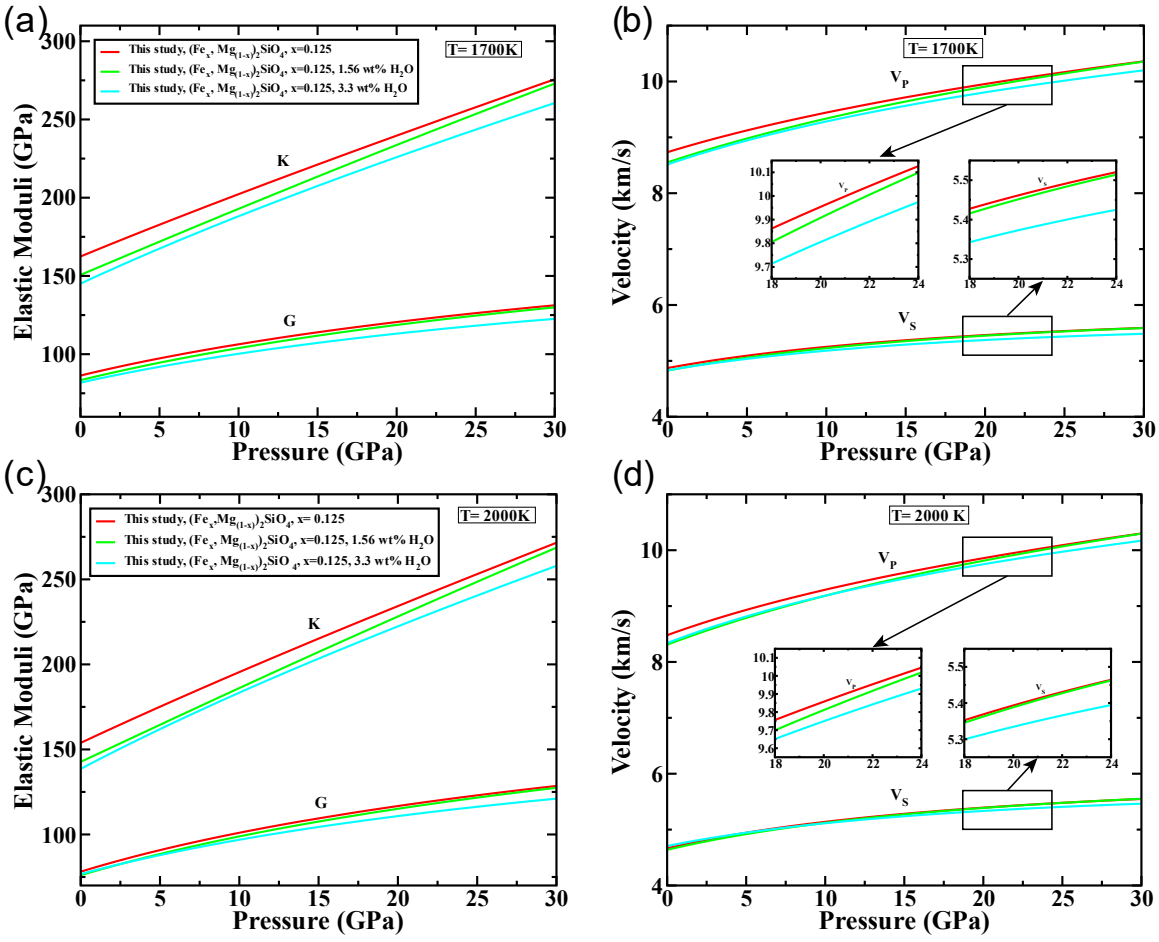

Figure 4: Our calculated elasticity of hydrous 12.5% Fe containing ringwoodite at 1700 K (top panel) and 2000 K (bottom panel). (a)&(c): Bulk (K) and shear (G) moduli; (b)&(d): Compressional (V_P) and shear (V_S) velocities as a function of pressure. The inset shows the zoomed-in portions of the V_P and V_S curves at pressures relevant to the stability field of ringwoodite.

The effect of higher temperature on the K, G, V_P, V_S of 3.3 wt.% H_2O containing ringwoodite is presented in Figure 4. Which shows that when the water concentration is as high as 3.3 wt.%, the pressure-induced suppression of the effects produced by water though present, is not significantly large enough.

A very interesting aspect that emerged out of our calculation is the contrasting behavior of the sound wave velocity curves for the two different hydrous ringwoodite samples. We find that at a given temperature, with the rise in pressure, the difference between the V_P and V_S of the hydrous and anhydrous phases in general decreases. The decrease is highly pronounced for the 1.56 wt.% H_2O containing ringwoodite, to the extent that at the pressures corresponding to the base of the MTZ, the sound wave velocities of the hydrous (1.56 wt.%) and anhydrous structures almost become indistinguishable. However, for the 3.3 wt.% water-containing model, its sound wave velocities are still distinctly different from the anhydrous ones at pressures relevant to the lowermost part of the MTZ. The reason behind such starkly different behavior of the two hydrous ringwoodite structures, namely 1.56 wt.% H_2O containing ringwoodite and 3.3 wt.% H_2O containing ringwoodite can be explained as follows: The presence of the vacant site in the hydrous ringwoodite allows the structure to be highly compressible at low pressures. However, as pressure increases, there is a reduction in the volume of the vacant octahedral site. This ends up having an adverse effect on the compressibility of the vacant site. It may be noted, that though the incorporation of protons takes care of the charge neutrality in the global sense, there still persists tiny charges on the oxygen atoms of the vacant octahedra at the microscopic level. Compaction of the vacant octahedral sites brings these charged oxygen atoms very close to each other, which leads to large coulomb repulsion. As a result, the vacant site cannot be compressed beyond a certain limit. In the case of 1.56 wt.% H_2O containing ringwoodite, which has single vacancies per unit cell, this limit is achieved at pressures relevant to the lower part of the MTZ. However, for the 3.3 wt.% water containing ringwoodite, since it has double the number of vacancies, and hence a greater ability to embrace compaction, the limit would be attained at a much greater pressure, way beyond the stability field of ringwoodite. A very pertinent question in this respect is the role played by Fe in modulating the influence of pressure on the hydration-induced reduction of the sound wave velocity of ringwoodite. Our calculations indicate that Fe to a certain extent subdues the “pressure effect”.

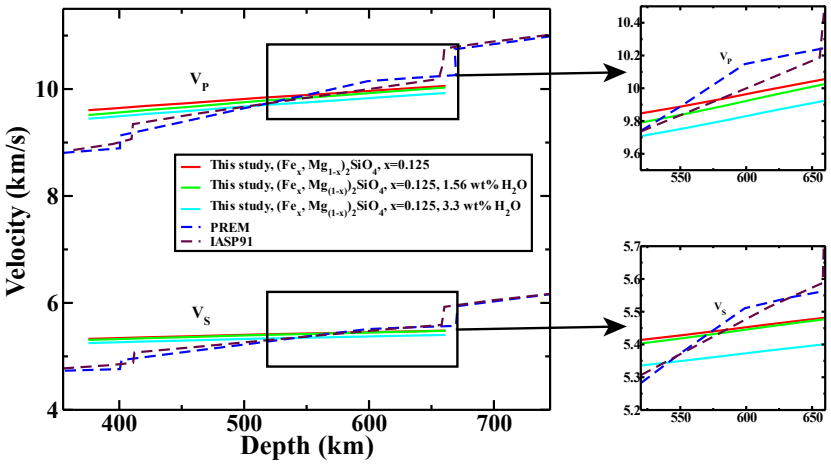

Figure 5: The compressional (V_P) and shear (V_S) velocities for 12.5% Fe containing anhydrous and hydrous (1.56 wt.% and 3.3 wt.% H_2O) ringwoodite as a function of depth along a mantle geotherm (Brown and Shankland, 1981).

Till now, we have been concentrating on two specific temperatures, that correspond to the upper and lower limits for the MTZ, namely 1700 K and 2000 K. However, in reality, the temperature and pressure simultaneously vary with depth inside the Earth. In order to plot the sound wave velocities, namely, V_P and V_S along a mantle geotherm, to decipher the ability of sound wave velocities to detect water in the MTZ. In this respect, we have chosen the geotherm proposed by Brown and Shankland (1981) and plotted the V_P and V_S as a function of depth, as shown in Figure 5. Our calculations indicate that at around 520 km, which corresponds to the average distance at which wadsleyite transforms to ringwoodite inside the Earth, the V_P and V_S of the anhydrous phase is larger than the 1.56 wt.% H_2O containing ringwoodite by 0.57% and 0.20% respectively. The same at around 660 km are 0.20% and 0.08% respectively. However, for the 3.3 wt.% H_2O containing case, its V_P and V_S are lower than that of the anhydrous case by 1.31% and 1.48% at around 660 km, thereby indicating that seismic methods may be able to detect high water content (3.3 wt.%) even at depths corresponding to MTZ-lower mantle boundary.

5. Conclusions:

1. The most dominant method for the incorporation of water in ringwoodite involves vacancies at octahedral sites charge balanced by an appropriate number of protons.
2. Our calculations show that there is a “reduction” in the sound wave velocity of ringwoodite in the presence of water, but this “reduction” is suppressed with increasing pressure.
3. For the model containing 1.56 wt.% H_2O, the difference in the sound wave velocities compared to the anhydrous model is less than 0.3% at the 660 km boundary.
4. Whereas, the difference in the sound wave velocities for the 3.3 wt.% H_2O containing ringwoodite compared to the anhydrous model is 1.4% at 660 km.
5. Hence seismic waves may not effectively detect water in ringwoodite when H_2O content is less than 1.56 wt.%. However, they remain robust in detecting regions with very high water content (~3.3 wt.%).

6. References:

1. Kudoh, Y., Kuribayashi, T., Mizobata, H., Ohtani, E., 2000. Structure and cation disorder of hydrous ringwoodite, γ-$Mg_{1.89}Si_{0.98}H_{0.30}O_4$. Phys. Chem. Miner. 27, 474–479.
2. Frost, D., 2008. The upper mantle and transition zone. Elements 4, 171–176.
3. Pearson, D.G., Brenker, F.E., Nestola, F., McNeill, J., Nasdala, L., Hutchison, M.T., Matveev, S., Mather, K., Silversmit, G., Schmitz, S., Vekemans, B., Vincze, L., 2014. Hydrous mantle transition zone indicated by ringwoodite included within diamond. Nature 507, 221–224.
4. Inoue, T., Weider, D.J., Northrup, P.A., Parise, J.B., 1998. Elastic properties of hydrous ringwoodite (γ-phase) in Mg2SiO4. Earth Planet. Sci. Lett. 160, 107–113.
5. Kohn, W., Sham, L.J., 1965. Self-consistent equations including exchange and correlation effects. Phys. Rev. 140, A1133.
6. Kresse, G., Furthmüller, J., 1996. Efficient iterative schemes for ab initio total-energy calculations using a plane-wave basis set. Phys. Rev. B 54, 11169.
7. Perdew, J.P.; Burke, K.; Ernzerhof, M.,1996 Generalized gradient approximation made simple. Phys. Rev. Lett., 77, 3865.
8. Blöchl, P.E., 1994 Projector augmented-wave method. Phys. Rev. B 50, 17953.
9. Hubbard, J., 1963 Electron correlations in narrow energy bands. Proc. R. Soc. A 1963, 276, 238.
10. Wallace, D.C. Thermodynamics of crystals. John Wiley and Sons, Inc. USA 1972.
11. Jacobsen, S.D.; Symth, J.R.; Spetzler, H.; Holl, C.M.; Frost, D.J., 2004. Sound velocities and elastic constants of iron-bearing hydrous ringwoodite. Phys. Earth Planet. Inter. 143-144, 47-56.
12. Panero, W.R., 2010. First principles determination of the structure and elasticity of hydrous ringwoodite. J. Geophys. Res. 115, B03203.
13. Chatterjee, S.; Saha-Dasgupta, T.; Sengupta, S. 2012. Visualizing frozen point defect tracks in Fe-containing olivines. EPL 98**,** 29001.
14. Dziewonski, A.M., Anderson, D.L., 1981. Preliminary reference earth model. Phys. Earth Planet. Inter. 25, 97–356.
15. Togo, A.; Tanaka, I., 2015 First principles phonon calculations in materials science. Scr. Mater. 108, 1-5.
16. Luo, C.; Deng, X.; Wang, W.; Shukla, G.; Wu, Z.; Wentzcovitch, R.M., 2021 cij: a python code for quasiharmonic thermoelasticity. Comput. Phys. Commun. 267, 108067.
17. Qin, T.; Zhang, Q.; Wentzcovitch, R.M.; Umemoto, K., 2019 Qha: a python package for quasiharmonic free energy calculation for multi-configuration. Comput. Phys. Commun. 237, 199-207.
18. Ito, E.; Katsura, T. , 1989 A temperature profile of the mantle transition zone. Geophys. Res. Lett., 16, 425-428.
19. Das, T.; Chatterjee, S.; Saha-Dasgupta, T., 2022 First-principles study of water incorporation in Fe-containing wadsleyite. Phys. Earth Planet. Inter. 333, 106940.

Published Paper: https://doi.org/10.1016/j.pepi.2024.107156

Acknowledgments:

I am thankful to the members of computational mineral physics lab. Financial support and access to computing facilities provided by IISER Kolkata are also gratefully acknowledged.